



Open Archive TOULOUSE Archive Ouverte (OATAO)

OATAO is an open access repository that collects the work of Toulouse researchers and makes it freely available over the web where possible.

This is an author-deposited version published in : <http://oatao.univ-toulouse.fr/>
Eprints ID : 4699

To link to this article : DOI :10.1002/sia.3136

URL : <http://dx.doi.org/10.1002/sia.3136>

To cite this version :

Liu, Y. and Laurino, A. and Hashimoto, T. and Zhou, X. and Skeldon, P. and Thompson, G.E. and Scamans, G.M. and Blanc, Christine and Rainforth, W.M. and Frolich, M.F. (2010) *Corrosion behaviour of mechanically polished AA7075-T6 aluminium alloy*. Surface and Interface Analysis, vol. 42 (n° 4). pp.185-188. ISSN 0142-2421

Any correspondence concerning this service should be sent to the repository administrator: staff-oatao@inp-toulouse.fr.

Corrosion behaviour of mechanically polished AA7075-T6 aluminium alloy[†]

Y. Liu,^a A. Laurino,^b T. Hashimoto,^a X. Zhou,^{a*} P. Skeldon,^a G. E. Thompson,^a G. M. Scamans,^c C. Blanc,^b W. M. Rainforth^d and M. F. Frolish^d

In the present study, the effects of mechanical polishing on the microstructure and corrosion behaviour of AA7075 aluminium alloy are investigated. It was found that a nano-grained, near-surface deformed layer, up to 400 nm thickness, is developed due to significant surface shear stress during mechanically polishing. Within the near-surface deformed layer, the alloying elements have been redistributed and the microstructure of the alloy is modified; in particular, the normal MgZn₂ particles for T6 are absent. However, segregation bands, approximately 10-nm thick, containing mainly zinc, are found at the grain boundaries within the near-surface deformed layer. The presence of such segregation bands promoted localised corrosion along the grain boundaries within the near-surface deformed layer due to microgalvanic action. During anodic polarisation of mechanically polished alloy in sodium chloride solution, two breakdown potentials were observed at -750 mV and -700 mV, respectively. The first breakdown potential is associated with an increased electrochemical activity of the near-surface deformed layer, and the second breakdown potential is associated with typical pitting of the bulk alloy.

Keywords: AA7075 aluminium alloy; corrosion; near-surface deformed layer; grain boundary

Introduction

Nano-grained, near-surface deformed layers are developed during hot and cold rolling, and by mechanically grinding or machining of aluminium surfaces, due to the high levels of surface shear strain imposed.^[1–5] The authors' recent work has revealed that mechanical grinding can generate a near-surface deformed layer on AA6111 aluminium alloy, and subsequent heat treatment to simulate paint baking processes results in preferential nucleation and growth of Q phase precipitates at grain boundaries within the near-surface deformed layer, giving dramatically increased corrosion susceptibility compared with the bulk microstructure.^[5] In a further study of mechanically polished AA7075 aluminium alloy by Zhao and Frankel, a double breakdown potential during anodic polarisation of the alloy in sodium chloride solution was observed.^[6,7] The first breakdown is attributed to the presence of near-surface deformed layers.

In the present study, the corrosion behaviour of mechanically polished AA7075 aluminium alloy has been investigated using electrochemical and electronoptical approaches.

Experimental

AA7075-T6 (Zn 5.1–6.1 wt%, Mg 2.1–2.9 wt%, Fe 0.5 wt%, Si 0.4 wt%, Cu 1.2–2.0 wt%, Mn 0.3 wt%, Cr 0.18–0.28 wt%, Ti 0.2 wt%, Al remaining) aluminium alloy sheet was used in the present study. Specimens were mechanically ground with 400, 800, 1200 and 4000 grit SiC paper, respectively, and then polished sequentially using 6, 3 and 1 μm diamond paste. The specimens were cleaned ultrasonically in an acetone bath and dried in a cool air stream before electrochemical measurement. Further specimens were prepared by etching in 10 wt% NaOH solution in order to remove the near-surface deformed layer generated during alloy fabrication.^[5,8]

Both mechanically polished and caustic-etched specimens were anodically polarised at 0.2 mV s⁻¹ in a deaerated 0.5 M NaCl solution. A relative large platinum foil was used as the counter electrode and an saturated calomel electrode (SCE) was employed as reference electrode.

Specimens before and after anodic polarisation were examined using a Carl Zeiss EVO 50 scanning electron microscope (SEM), and JEOL 2000 FXII and FEI F30 Tecnai transmission electron microscopes (TEMs). For TEM, ultramicrotomed sections, of nominal thickness 15 nm, generated with a diamond knife on a Leica Ultracut ultramicrotome, were examined.

Results and Discussion

Figure 1 illustrates the bright-field and dark-field images of the surface/near-surface region of AA7075 T6 aluminium alloy that had been mechanically polished. A near-surface deformed layer

* Correspondence to: X. Zhou, Corrosion and Protection Centre, School of Materials, The University of Manchester, PO Box 88, Manchester M60 1QD, United Kingdom. E-mail: xiaorong.zhou@manchester.ac.uk

a Corrosion and Protection Centre, School of Materials, The University of Manchester, PO Box 88, Manchester M60 1QD, United Kingdom

b CIRIMAT, ENSIACET, UMR CNRS 5085, 118 route de Narbonne, 31077 Toulouse Cedex 4, France

c Innoval Technology, Beaumont Close, Banbury, Oxon OX16 1TQ, United Kingdom

d Department of Engineering Materials, The University of Sheffield, Sir Robert Hadfield Building, Mappin Street, Sheffield S1 3JD, United Kingdom

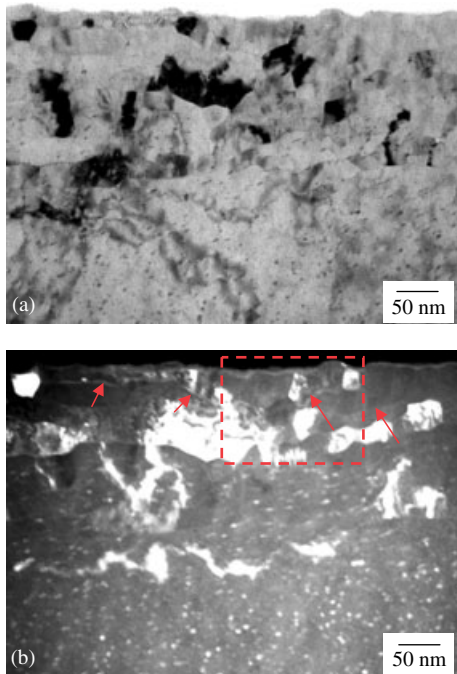


Figure 1. Transmission electron micrographs of an ultramicrotomed cross section of the surface/near-surface region of an AA7075 T6 aluminium alloy that had been mechanically polished to 1 μm diamond paste finish, revealing a near-surface deformed layer: (a) bright-field image; (b) dark-field image.

of 100–150 nm thickness, characterised by ultrafine grains, is revealed. The thickness of near-surface deformed layer varies across the alloy surface, with a maximum thickness of 400 nm. Further, hardening precipitates, approximately 5-nm diameter, typical for T6 alloy, are evident in the bulk alloy, as shown in both bright- and dark-field images, but are absent within the deformed layer. Interestingly, the dark-field image of Fig. 1(b) reveals narrow light bands of a few nanometres thickness within the deformed layer, as indicated by arrows.

A high angle annular dark-field (HAADF) image of the framed area in Fig. 1 is shown in Fig. 2(a). The HAADF image clearly reveals bright bands at the grain boundaries, indicating the presence of relatively heavy elements compared with the adjacent matrix.

Energy dispersive X-ray (EDX) analysis gives enhanced zinc and magnesium yields at the narrow bright bands at grain boundaries compared with the adjacent matrix (Fig. 2(b)). The absence of typical hardening precipitates and the presence of the narrow zinc- and magnesium-rich bands suggest dissolution of hardening precipitates and redistribution of alloying elements within the highly strained near-surface region during mechanical polishing.

Figure 3 shows transmission electron micrographs of an ultramicrotomed section of the AA7075 T6 aluminium alloy that had been etched in 10 wt% NaOH solution. A relatively uniform air-formed oxide film, of approximately 5-nm thickness, is present at the alloy surface. The hardening precipitates are evident in the bulk alloy beneath the air-formed film. The nano-grained, near-surface deformed layer shown in Fig. 1 is absent. The curved profile of the alloy surface reflects the typical scalloped texture of aluminium alloy after caustic etching.^[9]

Anodic polarisation curves of the AA7075 T6 aluminium alloy in 0.5 M NaCl solution after: (a) mechanically polishing to 1 μm diamond paste finish and (b) etching in 10 wt% NaOH solution

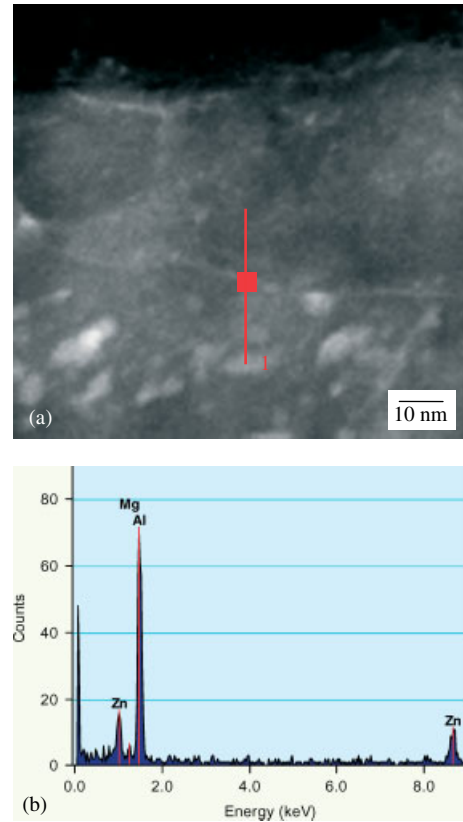


Figure 2. (a) High angle annular dark-field image of the framed area in Fig. 1; (b) EDX spectrum obtained at a grain boundary.

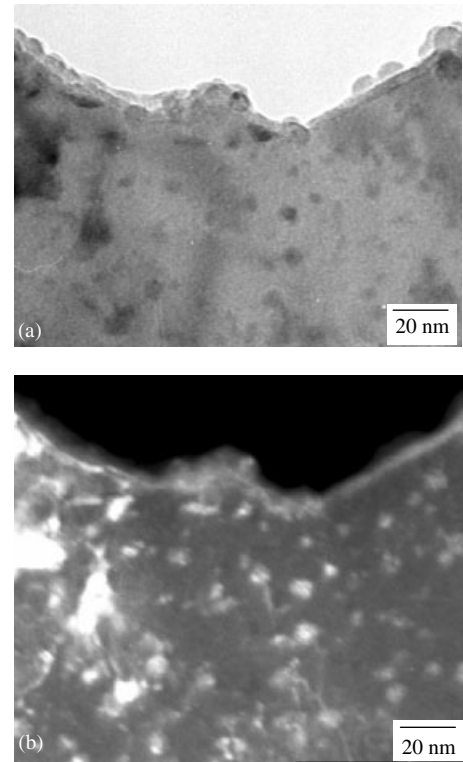


Figure 3. Transmission electron micrographs of an ultramicrotomed section of the surface/near-surface region of an AA7075 T6 aluminium alloy that had been etched in 10 wt% NaOH solution: (a) bright-field image; (b) dark-field image.

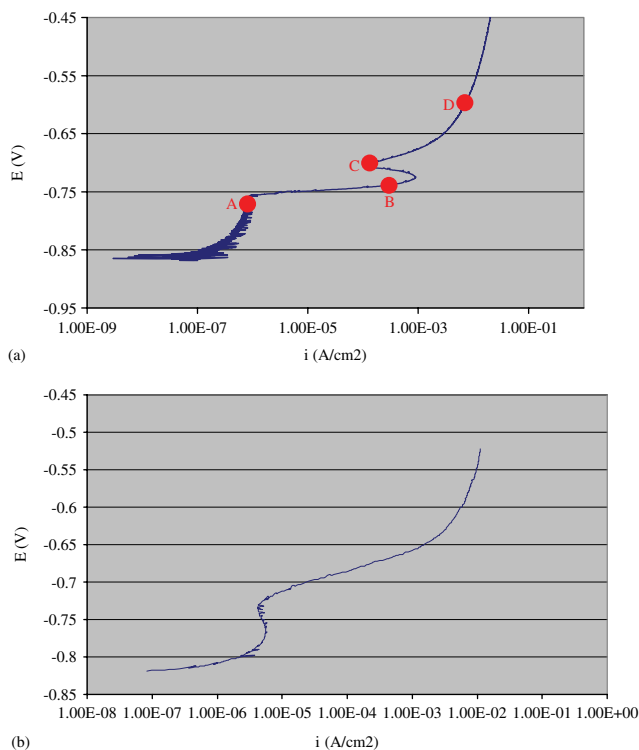


Figure 4. Anodic polarisation curves of AA7075 T6 aluminium alloy in 0.5 M NaCl solution: (a) mechanically polished to 1 μm diamond paste finish; (b) etched in 10 wt% NaOH solution.

are presented in Fig. 4. For the mechanically polished specimen, two current surges were evident (Fig. 4(a)). At -750 mV , the current density surged from $1 \times 10^{-6}\text{ A cm}^{-2}$ to a maximum of approximately $1 \times 10^{-3}\text{ A cm}^{-2}$. The current density fell back to a value of about $1 \times 10^{-4}\text{ A cm}^{-2}$ before increasing rapidly again at around -700 mV . However, for the caustic-etched specimen, only one current surge is evident after the passive region (Fig. 4(b)).

In order to gain insight into the two breakdown potentials in the anodic polarisation curve of the mechanically polished alloy, *ex situ* examination of the alloy surfaces after anodic polarisation to various potentials around the two breakdown potentials, as indicated by letters in Fig. 4(a), was carried out using scanning electron microscopy. The SEM image of the alloy surface after anodic polarisation to potential A, within the passivation region and immediately prior to the first breakdown potential, is presented in Fig. 5(a). The surface appearance is identical to that in the as polished condition, revealing polishing marks, suggesting little attack of the alloy at this potential.

Figure 5(b) displays two contrasting areas on the surface of the alloy that had been anodically polarised to potential B, after the first breakdown potential and before the current reaches its maximum. Polishing marks are still evident within area A, indicating area of intact alloy surface. However, fine features are clearly evident within area B, suggesting significant reaction with the solution, which is responsible for the current surge.

The size of area A had reduced significantly when the potential reached point C; only very small, isolated regions of area A are evident, as shown in Fig. 5(c). This explains the current fall after its maximum. Figure 5(d) displays the surface appearance when the potential reaches point D. Typical pitting is evident on the alloy surface. Thus, typical pitting of the bulk alloy is responsible for the second current surge.

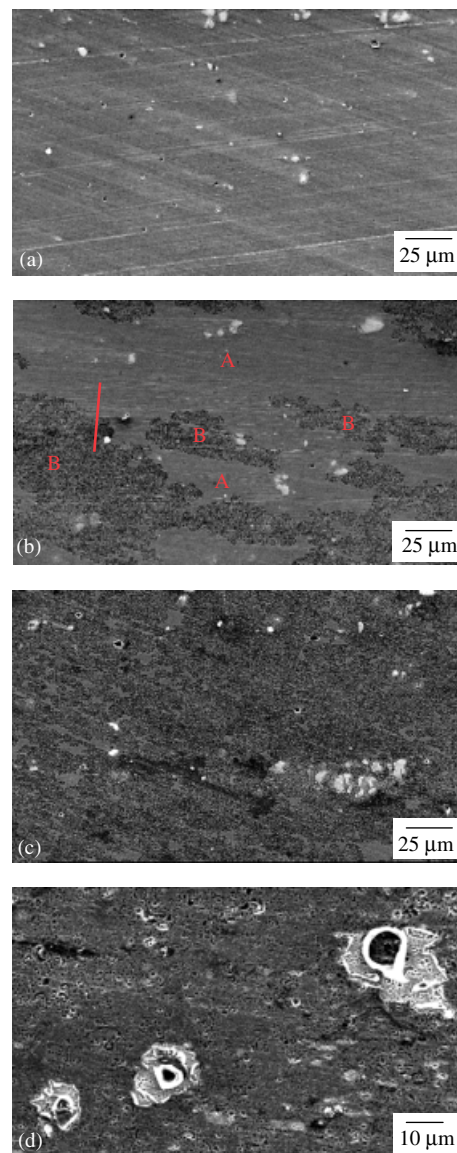


Figure 5. Scanning electron micrographs of an AA7075 T6 aluminium alloy that had been mechanically polished to 1 μm diamond paste finish and anodically polarised to various potentials indicated in Fig. 4, revealing surface appearance changes after anodic polarisation: (a) potential A; (b) potential B; (c) potential C; (d) potential D.

The previous suggestions are confirmed by transmission electron microscopy of the ultramicrotomed cross sections of the specimens shown in Fig. 5. A nano-grained, near-surface deformed layer of approximately 100 nm thickness is evident in the specimen that had been anodically polarised to potential A (Fig. 6(a)), showing little evidence of attack to the alloy, consistent with the scanning electron microscopy of Fig. 5(a). Further, a relatively uniform oxide film, of about 10-nm thickness, is present at the alloy surface. Clearly, the original air-formed film has thickened through the region of passivation.

Figure 6(b) illustrates a transmission electron micrograph of an ultramicrotomed section corresponding to Fig. 5(b). The section was taken from the boundary region between the areas A and B, with the sectioning position and direction being indicated by the solid line in Fig. 5(b). Within area A, again, a nano-grained, near-surface deformed layer is present above the bulk alloy. Within

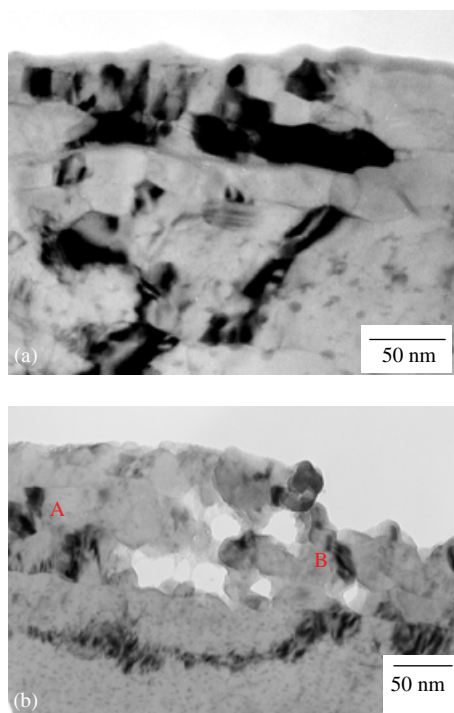


Figure 6. Transmission electron micrographs of ultramicrotomed sections of the surface/near-surface region of an AA7075 T6 aluminium alloy that had been mechanically polished to 1 μm diamond paste finish and anodically polarised to various potentials indicated in Fig. 4: (a) potential A; (b) potential B.

area B, severe localised corrosion is evident. The corrosion is intergranular and develops at, or adjacent to, grain boundaries. This is consistent with the surface appearance changes revealed by SEM in Fig. 5. However, the localised corrosion is confined within the near-surface deformed layer. The beneath bulk alloy appears intact.

Observation of the specimen surface during anodic polarisation revealed regions of changed appearances, i.e. from shiny to dull which appeared initially at the beginning of the first current surge and then spread rapidly as polarisation progressed. Such a surface appearance change is caused by the preferential attack of near-surface deformed layer, as revealed in Figs 5 and 6. The rapid spread of the attack of the near-surface deformed layer leads to the first current surge. However, the availability of near-surface deformed layer declines as the attack progressed, leading the current to fall back after its maximum.

During mechanically polishing, severe plastic strain was introduced to the surface/near-surface region of the alloy. Such plastic strain is of sufficient magnitude to cause geometric dynamic recrystallisation, therefore, resulting in significant microstructure refinement,^[10] consequently, leading to the formation of a nano-grained near-surface deformed layer. Further, within the near-surface deformed layer, the alloying elements have been redistributed, where the normal MgZn_2 particles for T6 are dissolved. Segregation bands, approximately 10-nm thick, containing mainly zinc and magnesium, are formed at the grain boundaries within the near-surface deformed layer.

The most significant influence on corrosion susceptibility results from the formation of continuous zinc- and magnesium-rich segregation bands at grain boundaries in the near-surface layer. Such segregation bands have different electrochemical properties due to relatively high zinc and magnesium contents with respect to the adjacent matrix regions, of comparatively low zinc and magnesium contents. Consequently, the microgalvanic coupling between the segregation bands and the adjacent matrix provides driving force for localised corrosion, resulting in severe attack in the near-surface deformed layer when the alloy is exposed to aggressive environment such as sodium chloride solution.

Conclusions

- Mechanical polishing of AA7075 aluminium alloy introduces significant surface shear stress to the near-surface region of the alloy, leading to the development of a nano-grained, near-surface deformed layer.
- Within the near-surface deformed layer, the normal MgZn_2 particles for the T6 temper are absent. Segregation bands, approximately 10-nm thickness, containing mainly zinc and magnesium, are developed at the grain boundaries within the near-surface deformed layer.
- The presence of such segregation bands promoted localised corrosion along grain boundaries within the near-surface deformed layer due to microgalvanic action.
- During anodic polarisation of mechanically polished alloy in sodium chloride solution, two current surges were observed at -750 and -700 mV. The increased electrochemical activity of near-surface deformed layer is responsible for the first current surge, and typical pitting of bulk alloy is responsible for the second current surge.

Acknowledgements

The authors wish to thank the Engineering and Physical Sciences Research Council for provision of financial support for the LATEST Portfolio Partnership.

References

- [1] G. M. Scamans, A. Afseth, G. E. Thompson, X. Zhou, *Proceeding of 2nd International Conference on Aluminium Surface Science and Technology*, Manchester **2000**, p. 9.
- [2] H. Leth-Olsen, K. Nisancioglu, *Corros. Sci.* **1998**, *40*, 1179.
- [3] M. Fishkis, J. C. Lin, *Wear* **1997**, *206*, 156.
- [4] G. Plassart, M. Aucouturier, *Proceeding of 2nd International Conference on Aluminium Surface Science and Technology*, Manchester **2000**, p. 29.
- [5] Y. Liu, X. Zhou, G. E. Thompson, T. Hashimoto, G. M. Scamans, A. Afseth, *Acta Mater.* **2007**, *55*, 353.
- [6] Z. Zhao, G. S. Frankel, *Corros. Sci.* **2007**, *49*, 3064.
- [7] Z. Zhao, G. S. Frankel, *Corros. Sci.* **2007**, *49*, 3089.
- [8] X. Zhou, G. E. Thompson, G. M. Scamans, *Corros. Sci.* **2003**, *45*, 1767.
- [9] E. V. Koroleva, G. E. Thompson, G. Hollrigl, M. Bloeck, *Corros. Sci.* **1999**, *41*, 1475.
- [10] F. J. Humphreys, M. Hatherly, *Recrystallization and Related Annealing Phenomena*, Pergamon: Oxford, **1995**.